3D Self-Aligning, Polarization-Independent Fiber-to-Chip Couplers

Ramesh Kudalippalliyalil,[1,2,*] Trisha Chakraborty,[1,2] Thomas E. Murphy, [1,3] and Karen E. Grutter [2]

[1,2] *University of Maryland, Department of Electrical and Computer Engineering, 8223 Paint Branch Dr, College Park, MD 20742, USA*
[2] *Laboratory for Physical Sciences, 8050 Greenmead Dr, College Park, MD 20740*
[3] *University of Maryland, Institute for Research in Electronics and Applied Physics, 8279 Paint Branch Dr, College Park, MD 20740, USA*
[*] *rameshk@umd.edu*

Abstract: We demonstrate low-loss (< 1 dB), broadband (BW∼100 nm near $\lambda \sim 1550$ nm) and polarization-independent fiber-to-chip couplers using 3D nano-printed polymer structures on Si_3N_4-on-SiO_2 platform. © 2023 The Author(s)

1. Introduction

An efficient and scalable interface between optical fibers and photonic integrated circuits (PICs) is critical for enabling the widespread adoption of silicon photonic technologies. However, high-performance fiber-to-chip coupling is inherently challenging due to several constraints, including tight alignment tolerances, sensitivity to variations in fiber and chip dimensions, cost-effectiveness, and scalability for mass production [1]. Some common fiber-to-chip coupling techniques include using V-grooves, lensed fibers, tapered fibers, and grating couplers. Each of these techniques has some drawbacks due to their different levels of precision, cost, bandwidth, and complexity [2].

Recently, 3D-printed polymer structures have emerged as a promising solution for plug-and-play fiber-to-chip coupling. They are capable of efficiently coupling light into large cross-section polymer waveguides [3] and onto silicon grating couplers [4]. Here, we demonstrate a universal self-aligned adiabatic coupler that enables efficient fiber-to-chip coupling into nanophotonic waveguides using 3D nano-printed polymer structures. Our design exhibits polarization independence, broad bandwidth, and significant tolerance to fabrication imperfections and misalignments. Additionally, we present measurements of a coupler fabricated on Si_3N_4-on-SiO_2.

2. Design and Simulations

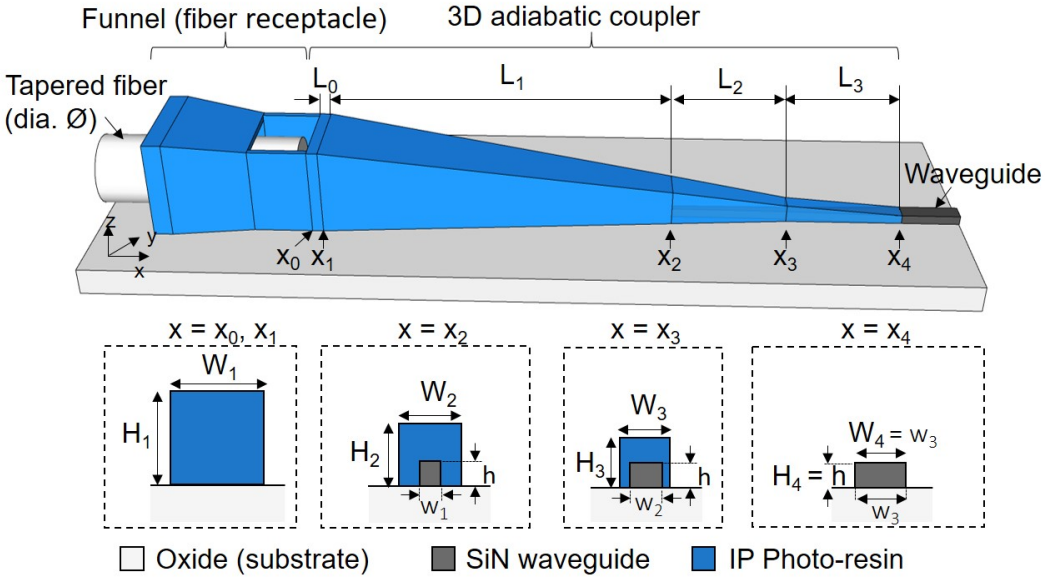

Fig. 1. 3D schematic of the fiber-to-chip coupler consisting of a funnel-shaped fiber receptacle, an input rectangular polymer waveguide (length - L_0) and three successive adiabatic tapers (lengths L_1, L_2 and L_3, respectively)). ∅ represents the input fiber diameter, W_{1-4} (w_{1-3}) and H_{1-4} (h_{1-3}) are the widths and heights of the polymer (Si_3N_4) waveguide at different cross-sections, x_1 to x_4 along the coupler.

Fig. 2 illustrates a schematic of the polymer-based 3D adiabatic coupler designed to couple light from a single-ended tapered single-mode fiber (diameter ~ 6 μm) to an output integrated Si_3N_4/SiO_2 waveguide (1.0 μm×0.5 μm). The tapered fiber is self-aligned when inserted into the funnel-shaped fiber receptacle [4], ensuring efficient coupling without active fiber alignment or stabilization. The coupler comprises four distinct sections: an initial straight section with a length denoted as L_0, followed by three linearly tapered regions with lengths L_1, L_2, and L_3. The second and third taper enclose and overlap the lateral inverse tapered on-chip waveguide. Cross-sections of the coupler at various locations are also shown in the figure.

In our design, we utilize the Ip-Dip2 photo-resin with a refractive index (n_{PR}) of 1.534 ($\lambda \sim 1550$ nm) for the 3D polymer structure. The input of the coupler is fixed to a square cross-section of 7.5 μm ×7.5 μm ($W_1 \times H_1$) over length $L_0 = 6$ μm. The inverse tapered Si_3N_4 ($n_{SiN} \sim 1.998$) waveguide has a fixed height of 500 nm and the width tapers from 0.2 μm to 0.35 μm and then to 1.0 μm over the lengths L_2 and L_3, respectively. The bottom cladding is 3 μm SiO_2 ($n_{ox} = 1.445$) and top cladding is air. The output Si_3N_4 waveguide supports both TE and TM fundamental modes. Using eigenmode expansion (EME) and finite-difference time domain (FDTD), we optimized the cross-sections and taper lengths of the 3D tapered polymer waveguide for maximum TE and TM transmission at the output. The optimized geometry of the 3D coupler is shown in Fig. 2 (a). Fig. 2 (b) and (c) show the electric field intensity profile along the length of the coupler, for TE and TM inputs, respectively. Fig. 2 (d) shows the calculated wavelength dependent transmission for TE ($95-97\%$) and TM ($93-96\%$) polarizations.

(a)

3D polymer (Waveguide)	L_0	$W_1 \times H_1$	L_1	$W_2 \times H_2$ ($w_1 \times h$)	L_2	$W_3 \times H_3$ ($w_2 \times h$)	L_3	$W_4 \times H_4$ ($w_3 \times h$)
Dimension (μm)	6	7.5 × 7.5	51	3.85 × 3.85 (0.2 × 0.5)	20	2 × 2 (0.35 × 0.5)	20	1 × 0.5 (1× 0.5)

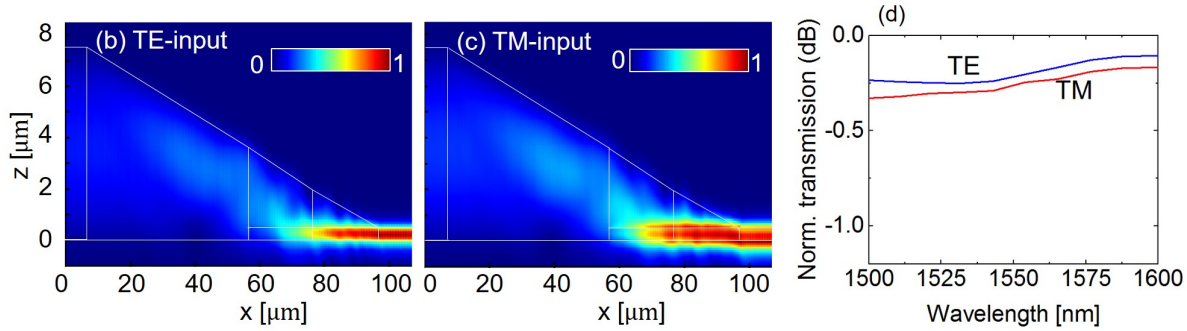

Fig. 2. (a) Optimized geometry of the 3D coupler. Electric field intensity profile along the length of the coupler for (b) TE and (c) TM inputs. (d) FDTD simulated transmission at the output of a Ip-Dip2/Si_3N_4 coupler.

3. Experimental Results

We first fabricate straight waveguides (3 mm long), input/output inverse tapers and ring resonators (radius 150 μm) in 500 nm thick LPCVD Si_3N_4 on 3 μm thick thermal SiO_2 using electron-beam lithography and inductively coupled plasma reactive ion etching. Device layouts were created with the CNST Nanolithography Toolbox [5]. Direct-laser writing based on two-photon polymerization of IP-Dip2 resin was used to define aligned 3D coupler structures. Additionally, we defined fiber receptacles at the coupler entrance, which secure the fiber and ensure proper alignment of the tapered fiber (Fig. 3 (c)). An SEM image of the fabricated 3D coupler is shown in Fig. 3(a).

Fig. 3(b) shows the optical characterization setup. Using micro-heater based fiber pulling system, we tapered a SMF-28 fiber to a diameter of 6 μm, then cleaved it at the taper waist to form two single-ended fiber tapers. The tapered input/output fibers were first inserted into the fiber entrance ports of the corresponding input/output 3D couplers on the device. This does not require high-precision active alignment, since the alignment is defined by the 3D structure (receptacle) itself. The tunable laser source (TLS) output (1525 nm $\leq \lambda \leq$ 1625 nm) is connected to the input tapered fiber through a free-space U-bench polarization controller, which includes two quarter-waveplates (QWPs) and one half-waveplate (HWP). The QWP-HWP-QWP configuration is used to set the desired polarization at the 3D coupler input. Given that the waveguide accommodates both TE and TM polarizations, we utilize the ring resonator spectrum as a polarization reference. This spectrum displays TE and TM resonances, each with distinct free spectral ranges (FSRs). We set the input polarization by adjusting the orientation of the wave plates to entirely suppress one of the TE or TM resonances, as shown in Fig. 3(d). In order to separate the loss of the adiabatic coupler from all unrelated contributions to the total insertion loss, we fabricated 3D diagnostic fiber receptacles (Fig. 3(c)(top)) and measured the tapered fiber-to-fiber transmission. We used this to normalize the measured transmission spectra in Fig. 3(d)-(f). Next, we measured the broadband transmission spectra of two different straight waveguides: one with optimal alignment with the 3D coupler and the other with intentional slight misalignment of ~ 0.5 μm in the y- and z-directions, relative

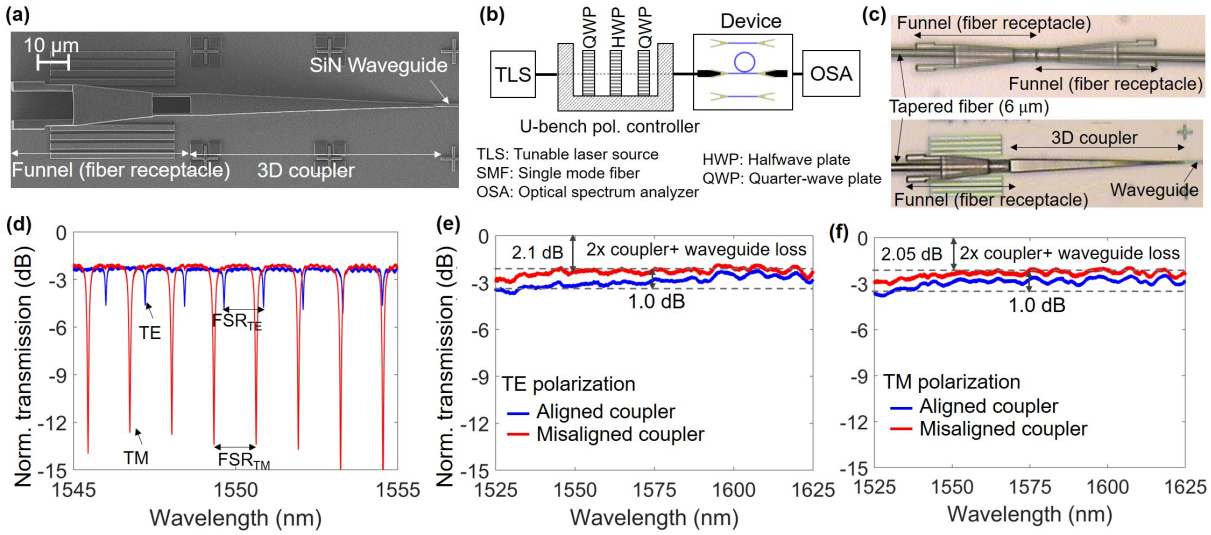

Fig. 3. (a) SEM image of the 3D adiabatic coupler. (b) Experimental setup. (c) Microscope images showing self-aligned fibers in the receptacle for tapered fiber-to-fiber coupling (top) and tapered fiber-to-3D coupler coupling (bottom). (d) Ring resonator transmission for TE and TM inputs. Transmission spectra of two different straight waveguides (3 mm long) with aligned and misaligned coupler, for TE (e) and TM (f) polarizations. The dotted lines represent the 1-dB limit of the spectra within the range of 1525 nm $\leq \lambda \leq$ 1625 nm.

to the waveguide. Both the TE (Fig. 3(e)) and TM (Fig. 3(f)) transmissions exhibit nearly wavelength-independent spectra with 1-dB bandwidths approaching 100 nm. The overall device loss (at $\lambda \sim 1550$ nm), encompassing both the input and output 3D couplers and the 3-mm long straight waveguide, is measured at approximately 2.1 dB for TE polarization and 2.05 dB for TM polarization, relative to the tapered fiber input. The propagation loss in the straight waveguide is approximately 1 dB/cm. This implies that the loss per 3D coupler is < 0.9 dB for each polarization. Additionally, the couplers exhibit significant misalignment tolerance, only around 1 dB additional loss for 0.5 μm (an easily achievable fabricated alignment precision) misalignment between the 3D coupler and the on-chip waveguide.

4. Conclusion

We designed and demonstrated a high-performance, self-aligning fiber-to-chip coupler using 3D nano-printed polymer structures. The demonstrated coupler exhibits a polarization independent loss of < 0.9 dB and a bandwidth close to 100 nm within the range of 1525 nm $\leq \lambda \leq$ 1625 nm. Additionally, the 3D coupler has a small footprint, measuring under 7.5 μm $\times$7.5 μm$\times$100 μm, and demonstrates significant tolerance to slight misalignment (less than 0.5 μm). The fibers are self-aligned in the input fiber receptacles without the need for active alignment tools. Furthermore, our Si_3N_4-on-SiO_2-based design allows for seamless integration onto diverse photonic platforms like silicon-on-insulator, AlN-on-insulator, and others, requiring only minimal tweaks to the design parameters. This versatility offers a promising solution for scalable packaging in future integrated photonics applications.

References

1. L. Ranno, P. Gupta, K. Gradkowski, R. Bernson, D. Weninger, S. Serna, A. M. Agarwal, L. C. Kimerling, J. Hu, and P. OBrien, "Integrated photonics packaging: challenges and opportunities," ACS Photonics **9**, 3467–3485 (2022).
2. R. Marchetti *et al.*, "Coupling strategies for silicon photonics integrated chips," Photonics Res. **7**, 201–239 (2019).
3. T. Chakraborty *et al.*, "Thermo-optic characterization of SU-8 at cryogenic temperature," in *2022 Conference on Lasers and Electro-Optics (CLEO),* (IEEE, 2022), pp. 1–2.
4. O. A. J. Gordillo *et al.*, "Plug-and-play fiber to waveguide connector," Opt. Express **27**, 20305–20310 (2019).
5. K. C. Balram, *et al.*, "The nanolithography toolbox," J. Res. National Inst. Stand. Technol. **121**, 464 (2016).